Q1 a)

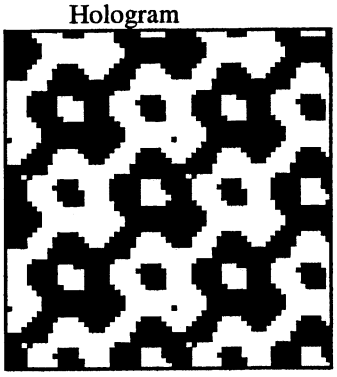

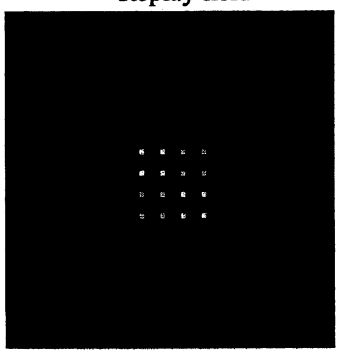

The hologram is an array of pixels in either phase or intensity which will generate a desired replay field. The relationship between the two is via the Fourier transform which converts one into the other and is reversible. The FT can be done by either a positive focal length lens or by going into the Fraunhopher region of free-space.

Assumptions: A perfect FT from the lens or free-space, perfect reproduction of the hologram on each pixels, no dead-space, no apodisation

If a pixellated pattern such as a grating is viewed from the end it can be modelled as a as a repetitive 1-D function. The repetition rate is defined by the pixel pitch or period.

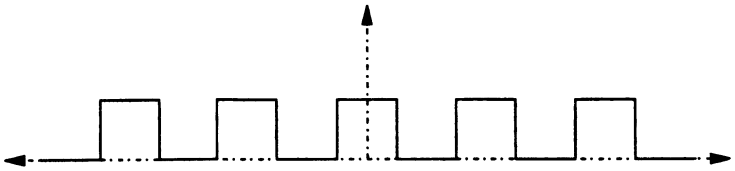

This can be expressed as a convolution of two functions.

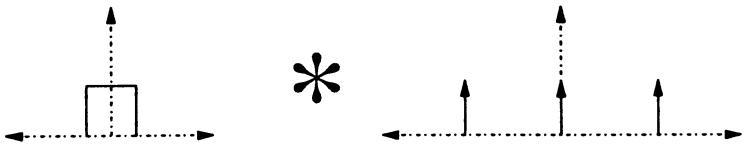

Where the delta function train represents the sampling or pixellation function and * represents a convolution. After the Fourier transform we have the replay field by Fourier analysis and the .

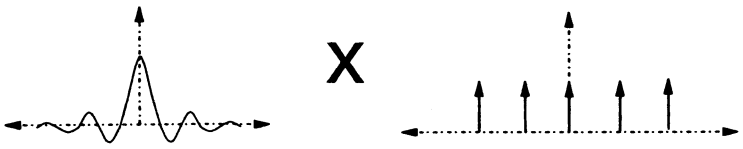

Gives the final result.

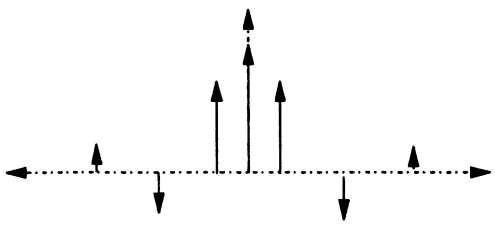

The train of delta functions has a sinc envelope and every second delta function is suppressed by the zeros of the sinc. Each symmetric pair of delta functions above represents a separate order and is repeated every odd harmonic.

b) i)

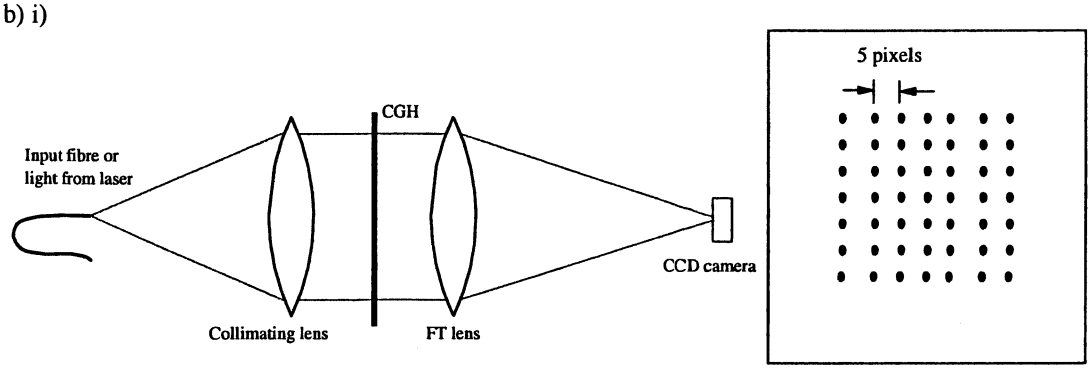

System layout Image on CCD (inverse)

ii) The square shape of the pixels in the CGH means that there will be an overall sinc (sine(x)/x) shaped envelope in the replay field.

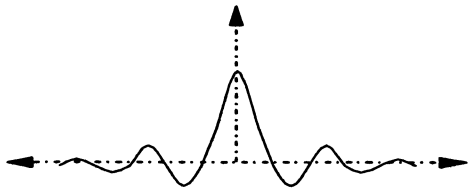

The original design of the CGH was to have all of the spots of equal height in the 7x7 array, however the outer spots will be reduced in height with respect to the central spot by the sinc envelope.

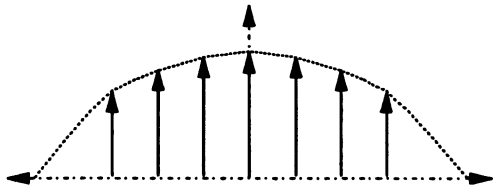

iii)
From the FT of a single pixel we have the envelope function for the CGH.
$F(u,v) = Aa^2\text{sinc}(\pi au)\text{sinc}(\pi av)$ which is in (u,v), normalised spatial frequencies.

We assume that for an NxN CGH we will have NxN spatial frequency positions in the central lobe of the sinc envelope in the replay field. We also assume no deadspace, apodisation and a perfect FT.

The position of the central spot in the replay field will be at (0,0) and the top rightmost spot will be at (17,17) in the replay field. In order to find the first zero of the sinc envelope (where $\text{sinc}(\pi) = 0$) we must have $(u,v) = 1/a$. Where a is the pixel pitch of the CGH. At the position $u = 1/a$, $v = 1/a$ we have the spatial frequency point of (128,128) hence the normalised co-ordinates will be at $(u,v) = (17/128a, 17/128a)$ which can be fed in the $F(u,v)$. This gives a ratio of 5.7% in height of the spots.

c) The DBS algorithm is not a good choice for designing this CGH as there it does not use the correct optimisation cost function. D uses a pure power difference in the replay field before and after pixel flips to define the cost function. This gives no control over the height of the spots in the replay field of the CGH, hence they will be uneven. This is especially the case if the sinc envelope has to be corrected for in the CGH.

A better algorithm is simulated annealing, however even this does not generate uniform replay fields, so a modified cost function is used based a round the difference between the spots desired and the average of the spots in the replay field.

Q2. a) If the optical system is split at this point, then the JTC just becomes two Fourier transforms and in fact can be done with a single laser, SLM and camera by doing two passes through the Fourier transform lens. This is know as the 1/f JTC.

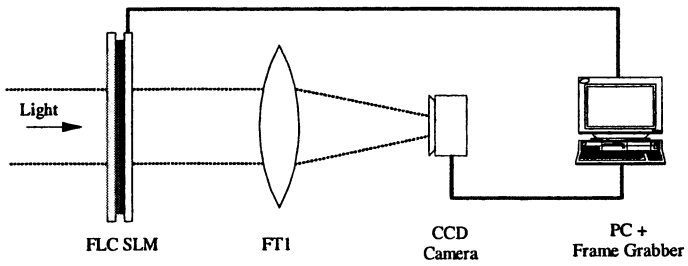

The input and reference images are displayed side by side on a FLC SLM as in a full JTC. The SLM is illuminated by a collimated laser beam and the images are Fourier transformed by a single lens in its focal plane. This spectrum is then imaged onto a CCD camera. The spectrum is then non-linearly processed before being displayed onto the SLM again to form the correlation information. The 1/f JTC is a two-pass system, using the same lens to perform the second Fourier transform.

If the spectrum was directly Fourier transformed, the result would be the two symmetrical correlation peaks characteristic of the JTC along with a huge zero order located in the centre of the output plane. The quality of the correlation peaks and the zero order can be improved by non-linearly processing the spectrum that also suits the available FLC SLM technologies. Some of the best results have been reported by using binary thresholds on the spectrum to improve the correlation peaks. A binarised spectrum produces good sharp correlation peaks and reduced zero order. If the binarised spectrum is converted to binary phase modulation [-1,+1], then the zero order can be reduced to around the height of the correlation peaks.

A variety of processing schemes have been tried. The first technique was to use a basic median threshold filter on the spectrum, but this gave a very poor bitwise average after the threshold to binary phase. A 3x3 convolution binarisation scheme was also tried and gave reasonable results, but the processing time was slow due to the complexity of the filtering algorithm. The success of this algorithm is due to fact that the 3x3 convolution is a form of edge enhancement, which enhances the spectrum and the noise in the dark areas. The best scheme used to binarise the spectrum was based on a nearest neighbour average comparison. The pixel to be binarised, P_{jk} is thresholded based on the average of its four nearest neighbours.

$$P_{j,k} = \begin{cases} +1 & \text{if} \quad P_{j,k} \geq \frac{1}{4}\left(P_{j-1,k} + P_{j+1,k} + P_{j,k-1} + P_{j,k+1}\right) \\ -1 & \text{Otherwise} \end{cases}$$

b) This is the basis of a head tracking system. A camera is mounted on the helmet of the pilot and is pointing at the cockpit area, hence the pilot's view of the cockpit is fed frame by frame to the correlator. Each frame is fed in sequence through the correlator, with the first frame being used as the reference and the next one as the input, then the next one becomes the reference and the third the input and so on... Thus motion between frames can be tracked as long as there is an overlap of common information in each frame from the helmet.

If the pilot's view (and therefore head position) does not change from one frame to the next, then the correlation between frames will be in the centre of the output plane. If the pilot's head rotates, then the view of the cockpit will shift from one frame to the next and the correlation peaks will also shift proportional to how much of the pilot's view has shifted from one frame to the next. This is shown below along with the correlations from an unshifted and shifted pair of frames.

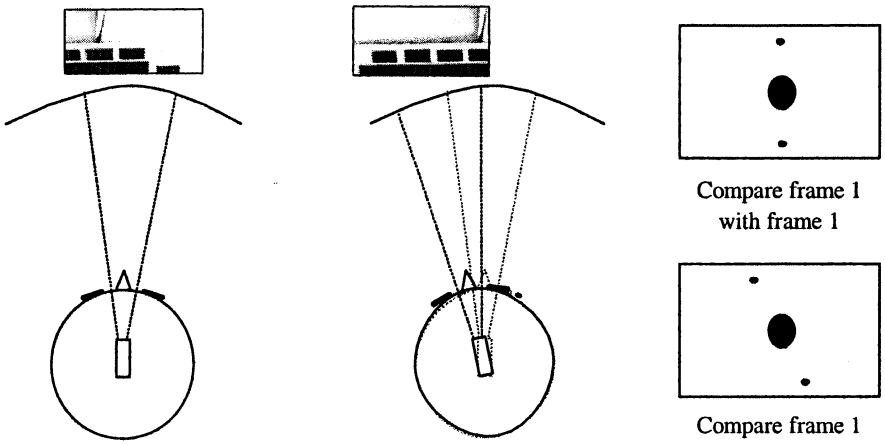

Frame 1 Frame 2

The position of the correlation peaks tells us how much one frame has moved from the previous one when the pilot's head rotates, hence by measuring the distance and knowing the dimension between the pilot and the cockpit, we can sense how much the head has rotated and therefore track it.

c) The view of the pilot from one frame to the next must overlap by more than 20% in order for the correlator to produce reliable peaks.

The 20° field of view of the camera corresponds to roughly 2*1.3*tan(20) = 0.45m of the cockpit panel. The 20% overlap area is 0.09m along the cockpit panel.

This corresponds to 90mm which is the maximum distance per correlation cycle along the cockpit panel the view can take before it goes beyond the 20% overlap limit.

The 90mm corresponds to a angular resolution of 4° about the pilot's head centre per correlation cycle.

If the correlator operates at 50 correlations per second, then the maximum angular speed of the pilots head must not exceed 200° per second (3.5 $rads^{-1}$) to keep track of the position.

d) When the pilot looks up through the canopy they will be looking at either the sky or the ground depending which way up they are. The sky is rather feature-less for correlation, hence the head tracker will be able to register the position of the pilot's view. If they are looking at the ground, then it will be moving wrt the canopy, hence it will confuse the correlation process.

The simplest solution is to make sure that the view of the camera on the pilot's head never leaves the cockpit console panel during any of the pilot's possible head positions, hence it will always have a fixed reference to correlate from frame to frame.

A second solution is to put a pattern on the canopy which can be picked up by the camera, but not by the pilot. Perhaps something holographic?

Q3 a) The term *loss* refers to the amount of optical power which is launched down the optical fibre at the output end of the switch. It is normally the ratio of the optical power launched into each output fibre and the optical power at each input fibre. If the switch is configured to route light to the *k*th fibre in an output array of *n*, then the *crosstalk* is the ratio of light launched down the desired fibre to the light launched down one of the other fibres which are not being routed. Both are normally expressed in decibels.

Fan-in loss arises in holographic switch because the only fibre in the output which is on axis is the one in the centre of the array. When light is steered to the outermost fibres it is at an angle to the central axis which no longer satisfies the perfect launch condition of a single mode fibre. Hence there is a loss which depends on this angle and therefore the position of the output port.

i) In a fibre to fibre switch, loss is a very important parameter as it will effect the overall efficiency of the optical fibre network and therefore the sensitivity of the receiver. The lower the loss the better. The crosstalk is also a critical parameter in a holographic switch as it defines the background noise in each fibre. The more fibres in the input of the switch, the more background there is and the more sensitive to crosstalk the switch will be.

ii) In the case of the shutter switch these parameters are not so critical. A shutter switch is normally used to connect lasers to photodetectors which have a much better sensitivity than a full fibre link receiver. Hence we can get away with much higher losses and higher crosstalks.

b) The total input power which appears in the output plane is P_{in}. The total power which is routed into a spot by the CGH is P_{sp} and the remaining power is dissipated into the whole plane as the background or noise power P_{bk}.

$$P_{in} = 2P_{sp} + P_{bk}$$

The factor of 2 is due to the symmetry of the pattern due to binary phase. We can define the CGH efficiency η as the ratio between the power in the spot, P_{sp} and the input power P_{in}.

$$\eta = \frac{P_{sp}}{P_{in}}$$

A typical value for this efficiency would be around 38% for a CGH generated by simulated annealing (the ideal maximum would be 50% due to the symmetry in the replay field). If the switch is configured to route light to the *k*th fibre in an array of *n*, then the crosstalk is the *ratio of light launched down the desired fibre to the light launched down one of the other fibres which are not being routed.* For *n* fibres in the output array of a 1 to *n* switch, the power into a single fibre will be ηP_{in}. If the CGH has *N*x*N* pixels, then the replay field can also be assumed to contain *N*x*N* 'spatial frequency pixels'. If we assume that the background power is uniformly distributed over the N^2 spatial frequency pixels in the replay field then the background power at each pixel will be.

$$P_{bpix} = \frac{(1-2\eta)P_{in}}{N^2}$$

Hence the crosstalk is the ratio of the light routed to a fibre to P_{bpix}.

$$C = \frac{\eta}{1-2\eta} N^2$$

The *n* x *n* analysis for the crosstalk is the same except that we now have the background noise from each of the other *n* - 1 input fibres appearing at the each output fibre along with the ηP_{in} from the routed input. Hence the crosstalk will be.

$$C = \frac{\eta}{1-2\eta} \frac{N^2}{(n-1)}$$

c) Any three of these will do...

- Due to the binary phase modulation, the distribution of the background power is not uniform and there tends to be small peaks of intensity which may occur at fibre positions. This becomes less of a problem with large numbers of CGH pixels and careful CGH design.
- The number of CGH pixels is finite and forms an overall aperture which leads to sinc or Bessel sidelobes on the individual spots. There is also Gaussian illumination. These effects lose power into the sidelobes and cause the spot to be broader than the original source fibre, leading to poor fibre launch efficiency (apodisation).
- The pixel pitch is finite which leads to an overall sinc envelope which reduces the power into spots that occur further away from the centre of the replay field. The sinc envelope also leads to power being lost in the outer orders due to replication of the replay field.
- The SLM used to display the CGH inevitably has deadspace (optically inactive areas) between the pixels. This space limits the performance of the CGH as it alters the envelope of the replay field and increases the power replicated into the unwanted higher orders.
- The physical alignment of the fibres in the output array is not perfect, so there are position errors in the spot locations which leads to poor interconnections. This can be corrected if *N* is large by slightly shifting the positions of the spots to match the fibre array.
- So far we have assumed perfect optics with no limitations or distortions. In reality, it is optically more difficult to route light into the outer corners leading to fan-in loss. This loss is usually modelled as a *1/n*. We can reduce this by placing the outputs close to the zero order and limiting *n*.

d) The single hologram *n* x *n* switch is limited in scalability as it can only diffract light over a limited angle given by the Bragg equation for a simple grating. We can rectify this by using two holograms to

steer the light. The first steer light into the switch, whilst the second steers light out of the switch back onto the output fibre's axis. The most efficient combination for routing is if the second hologram is the complex conjugate of the first routing hologram.

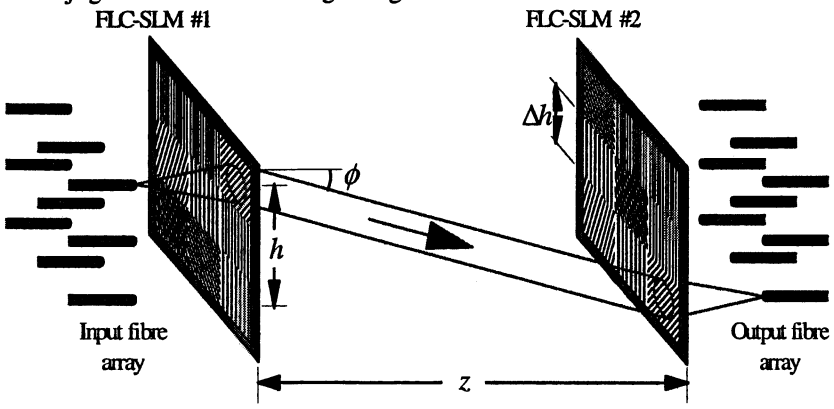

The two hologram switch can be scaled to any size and the loss through the switch does not scale with the number of input and output ports, it does however increase the loss as there are now two holograms routing the same beam. The only parameters which scale with the number of ports are the crosstalk and the physical length z. The crosstalk of the two hologram switch is greatly improved as the crosstalk of the first hologram is multiplied by the cross talk of the second hologram.

$$C = \left(\frac{\eta}{1-2\eta} \frac{N^2}{(n-1)} \right)^2$$

Q4 a) A mode is a discrete solution to the propagation of an optical signal along a waveguide structure. It is a function, distribution of energy, or propagation angle which can maintain propagation along a waveguide structure. This is normally through a process of TIR at the refractive index boundary which maintains the direction of propagation along the length of the fibre. A mode can only exist if it propagates in a stable fashion, hence any unstable energy fields will be lost from the waveguide structure.

In a single mode waveguide structure the conditions of propagation limit the umber of stable modes to one. Hence only the pure single mode function or condition will propagate. This is a very pure system of propagation, however it is also very restrictive in terms of wavelength cut-off and physical size of the waveguide. Multi-mode is where more that one mode is stable and so they can propagate together. This is a much more relaxed condition which may excite a few 10's of mode right through to thousands as found in a plastic optical fibre. There is a point when the number of modes is so numerous that it gives the illusion of any propagation being accepted.

Single mode waveguides are much more difficult to fabricate as they are usually very small dimensions to maintain the single mode operation. Single mode waveguides are usually 2-5um in size whereas multimode waveguides can be 100's of um across.

b) Maxwell's equations describe the characteristics of electromagnetic waves in terms of the electric (**E**) and magnetic fields (**H**), assuming a general form such that:

$$\tilde{\mathbf{E}} = \mathbf{E}(\mathbf{x},\mathbf{y}) e^{j(\omega t - \beta z)}$$

$$\tilde{\mathbf{H}} = \mathbf{H}(\mathbf{x},\mathbf{y}) e^{j(\omega t - \beta z)}$$

where (x,y) denotes a plane transverse to the z axis. Hence we can express Maxwell's equations, assuming $\mu = \mu_0$ and $\varepsilon = \varepsilon_0 n^2$,

$$\nabla \times \tilde{\mathbf{E}} = -\mu_0 \frac{\partial \tilde{\mathbf{H}}}{\partial t}$$

$$\nabla \times \tilde{\mathbf{H}} = \varepsilon_0 n^2 \frac{\partial \tilde{\mathbf{E}}}{\partial t}$$

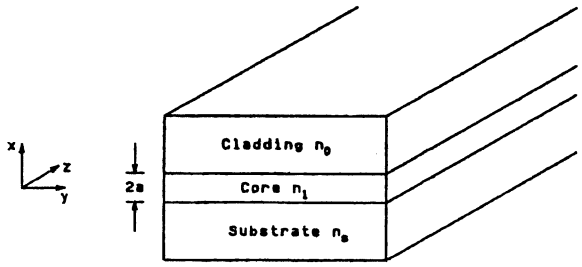

In a slab waveguide such as that shown above, the electromagnetic fields E and H do not have a y dependency due to the geometry of the waveguide. Hence we set $\partial \mathbf{E}/\partial y = 0$ and $\partial \mathbf{H}/\partial y = 0$. Putting these relationships into the ones above gives us two independent electromagnetic modes denoted as the transverse electric TE and transverse magnetic TM modes.

We can also use these wave equations along with the boundary conditions of the waveguide to derive the propagation constants and the dispersion equations (often called eigenvalue equations). If we consider the act that the guided EM fields are confined in the core and will exponentially decay in the cladding, then the electric filed distribution will be:

$$E_y = \begin{cases} A\cos(\kappa a - \phi)e^{-\sigma(x-a)} & (x > a) \\ A\cos(\kappa a - \phi) & (-a \le x \le a) \\ A\cos(\kappa a + \phi)e^{\sigma(x+a)} & (x < -a) \end{cases}$$

The theory for rectangular waveguides can also be used to derive solutions of Maxwell's equations for optical fibres. In this case the circular symmetry of the fibre makes analysis possible. The EM field can be expressed in cylindrical coordinates as

$$\tilde{\mathbf{E}} = \mathbf{E}(r,\theta)e^{j(\omega t - \beta z)}$$

$$\tilde{\mathbf{H}} = \mathbf{H}(r,\theta)e^{j(\omega t - \beta z)}$$

In axial symmetric fibres, the refractive index is independent of θ, $n(r)$. The simplest waveguide structure is the step index fibre, with a core radius of a, made from material n_1 and cladding made from material n_0.

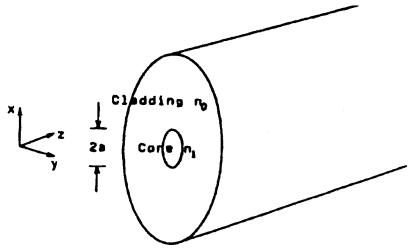

c) The analysis of Maxwell's equations for rectangular waveguides is useful for simple structures, but does not help when considering more complex systems such as couplers or Mach Zehnder devices. There are several more general techniques based on finite element and finite difference analysis which can be used to solve these more complex structures.

One of the most common is the beam propagation method (BPM), of which there are two types, the fast Fourier transform method and the finite difference method. Both techniques rely on separating the propagation of the EM wave into slow and fast varying components which can be solved separately and propagated through a finite element mesh. These techniques are often not totally rigorous, but are

sufficiently accurate to describe the basic wave properties. A typical simulation of a waveguide s-bend is shown below.

d) Another exciting wavelength selective waveguide device is the array waveguide generator (AWG) which is an integrated waveguide device which can mutiplex/demultiplex multiple wavelength channels simultaneously. The structure of an AWG is shown in the figure below.

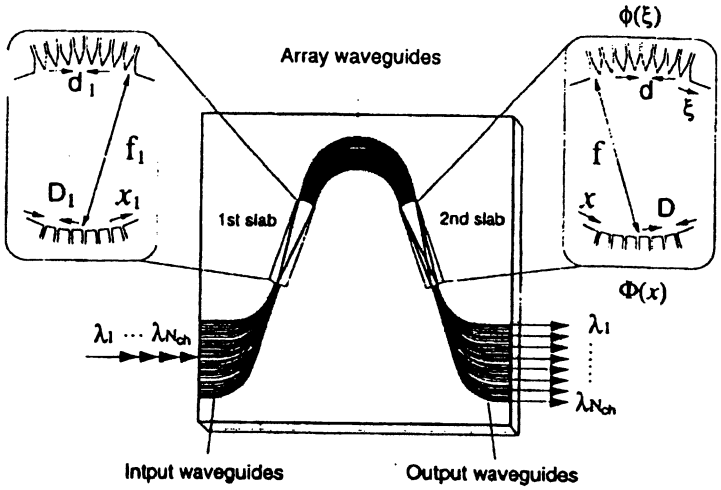

The device consists of several input channels and an array of output channels which matches the number of discrete wavelengths in the WDM system (normally 16 or 32). The input waveguides will contain channels which may contain any or all of the WDM channels. The input is launched in the slab waveguide which spreads the modes out in the y axis onto a further series of S/M waveguides. These are connected to the output slab section via a series of paths of increasing length. This is like passing the input channels through a linear phase ramp or perfect grating. The output slab section then allows the modes to propagate further onto the output waveguides. The effect of the two slabs and the phase ramp is to separate the WDM channels so that each one is launched into its own output waveguide. This is effectively demultiplexing the WDM channels, and the process can be reversed to multiplex the channels as well into one output.

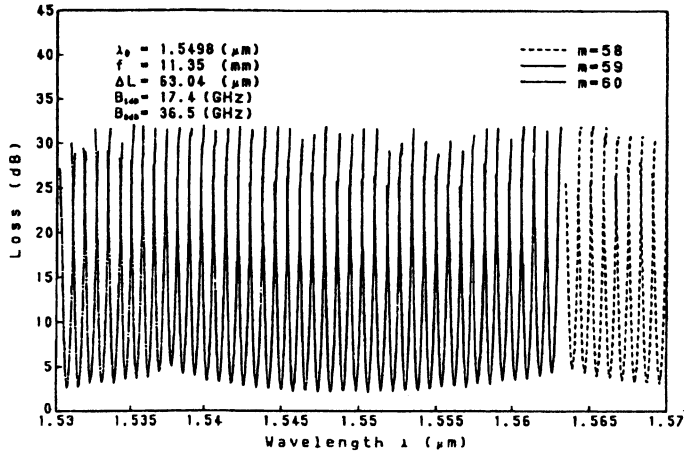

The plot above shows how 32 WDM channels have been separated into individual WDM output waveguides. Once again the whole process can be analysed using the same Fourier analysis as used with holograms as the slab areas operate in a similar manner to free space diffraction. The archilles heel of the AWG is that the tolerances on fabricating the waveguides are extremely high as the path lengths have to be exactly right for low loss and crosstalk. The AWG can be further enhanced by adding phase modulators into each of the arms creating a tuneable AWG.